type +4, +3). It is certainly this electrostatic factor that contributes most to the observed difference in rate (100-fold) of this outer-sphere reaction in the two media.

Acknowledgment. We are grateful to the DAAD (Deutscher Adademischer Austauschdienst) for a fellowship to C.M. and to the Universidad de Concepcion for partial support to C.M.

Registry No. $Mo_2O_4^{2+}$, 40804-49-7; $Mo_2O_2S_2^{2+}$, 52700-51-3; $Fe(H_2O)_6^{3+}$, 15377-81-8; $Fe(phen)_3^{3+}$, 13479-49-7; $Mo_3O_4^{4+}$, 74353-85-8.

Contribution from the School of Chemistry, Georgia Institute of Technology, Atlanta, Georgia 30332, and Istituto di Teoria e Struttura Elettronica, Consiglio Nationale della Ricerche, 00016 Monterotondo Stazione, Roma, Italy

Spectroelectrochemistry of a μ-Nitrido-Bridged Iron Phthalocyanine Dimer

LAWRENCE A. BOTTOMLEY,*† JEAN-NOEL GORCE,† VIRGIL L. GOEDKEN,‡ and CLAUDIO ERCOLANI‡

Received May 30, 1985

The synthesis of (μ-nitrido)bis[(phthalocyaninato)iron(III$^1/_2$)], $[(Pc)Fe]_2N$, has been achieved, and its physicochemical properties have been determined. The electrochemistry of $[(Pc)Fe]_2N$ was studied in neat pyridine at a Pt-button electrode. One single-electron-oxidation and three single-electron-reduction processes were observed for the dimer within the accessible potential window of the solvent-supporting electrolyte system. Variable potential sweep rate cyclic voltammetric experiments verified the chemical reversibility of the oxidation and reduction processes at short times. Coulometry confirmed that the first oxidation and first reduction steps each involved the passage of 1 equiv of charge/dimer. Spectra taken on the electrogenerated dimer cation and anion verified complete retention of the single-atom bridging moiety. The other electron transfers resulted in the decomposition of the dimer. An electron-transfer pathway based upon the combined voltammetric, spectroelectrochemical, and coulometric results is proposed and compared to that observed for the analogous porphyrin complex (μ-nitrido)bis[(tetraphenylporphinato)iron(III$^1/_2$)], $[(TPP)Fe]_2N$.

Introduction

Until recently, the μ-nitrido dimer of iron tetraphenylporphyrin, $[(TPP)Fe]_2N$, represented the only well-characterized example of an N-bridged complex containing two first-row transition-metal atoms. The physicochemical properties of this complex have been the subject of considerable interest.[1-5] Its electronic structure has been examined, and an orbital diagram that accounts for the observed structural and magnetic properties has been constructed.[6]

The surprising stability of the μ-nitrido complex, $[(TPP)Fe]_2N$, suggested that, in general, μ-nitrido bridges might be more stable than previously thought. Accordingly, we have sought to synthesize and characterize related species in order to place the $[(TPP)Fe]_2N$ complex within a general framework of μ-bridged and μ-nitrido-bridged complexes.[7,8] The obvious similarities between porphyrins and phthalocyanines (dianionic charge, tetraaza donor atoms, aromatic planar ligand skeleton) suggested the μ-nitrido complex of (Pc)Fe as the most reasonable starting place to synthesize other nitrido dimers. The thermal decomposition of $(TPP)Fe(N_3)$ was the route used for the synthesis[1a] of $[(TPP)Fe]_2N$. As previously described[9], the thermal decomposition of NaN_3 in boiling α-chloronaphthalene in the presence of (Pc)Fe produced $[(Pc)Fe]_2N$. Although not isolated and definitely characterized, a similar $(Pc)Fe(N_3)^-$ derivative is very likely present as an unstable intermediate in the preparation of $[(Pc)Fe]_2N$.

Unlike $[(TPP)Fe]_2N$, $[(Pc)Fe]_2N$ is highly insoluble in nondonor solvents and only sparingly soluble in donor solvents such as nitrogenous bases. This property severely impedes studies of the physical properties of this complex. The aim of the present study was mainly devoted to the exploration of the physicochemical properties of $[(Pc)Fe]_2N$ in pyridine and to compare these properties with those determined for $[(TPP)Fe]_2N$ under identical conditions.

Experimental Section

Materials. $[(TPP)Fe]_2N$ was synthesized by the method of Summerville and Cohen.[1a] Solid samples of $[(TPP)Fe]_2N$ were slowly oxidized in air over the course of several weeks. Pure $[(TPP)Fe]_2N$ was obtained by the following chromatographic procedure. A saturated solution of the crude material in CH_2Cl_2 was prepared and applied to a column of freshly activated basic alumina. Elution with CH_2Cl_2 yielded a fast moving greenish red band, which was identified as the μ-oxo dimer by its characteristic visible spectrum. Gradient elution (from 0.0 to 100%) with freshly distilled tetrahydrofuran (THF) produced a dark red band. Spectral measurements identified this fraction as pure $[(TPP)Fe]_2N$. Elution with 1:9 methanol/THF yielded the dimeric cation, $([(TPP)Fe]_2N)^+$. This material was reduced to the neutral compound either by electrochemical means or by treatment with a deoxygenated aqueous solution of sodium dithionite.

(Pc)Fe was purchased from Eastman Kodak and purified by vacuum sublimation to remove insoluble oxide impurites. In a typical preparation of $[(Pc)Fe]_2N$, 1.0 g of (Pc)Fe was placed in 20 mL of α-chloronaphthalene and heated to the boiling point of 265 °C. A large excess, 1.0 g, of NaN_3 was added with constant stirring for 1 h. During this period, N_2 gas evolved and the color of the solution changed from the typical blue-green of (Pc)Fe to the pure dark blue-purple of the suspended product. Because the reaction is heterogeneous, it is difficult to determine visually when the reaction is complete. Reaction progress was monitored by taking small aliquots of the reaction mixture, filtering the sample, washing the filtrate with water and methanol, and then drying the sample. The IR spectrum measured for material treated in this fashion was then examined for the disappearance of the N_3^- absorption and the appearance of the antisymmetric Fe–N–Fe absorption, which is one of the most intense in the spectrum. After the reaction was completed, the reaction mixture was cooled and the product filtered, washed with chloroform (to remove α-chloronaphthalene), alcohol, and finally water (to remove any excess N_3^- and other water-soluble impurities), and then dried under vacuum; yield 90%. Anal. Calcd for $Fe_2C_{64}H_{32}N_{17}$: C, 66.80; H, 2.80; N, 20.69. Found: C, 66.68; H, 2.85; N, 20.51.

In a typical preparation of $[(py)(Pc)Fe]_2N)PF_6$, a suspension of $[(Pc)Fe]_2N$ in chloroform and a solution of 1.0 g of oxidant (e.g. ferro-

(1) (a) Summerville, D. A.; Cohen, I. A. *J. Am. Chem. Soc.* **1976**, *98*, 1747–1752. (b) Scheidt, W. R.; Summerville, D. A.; Cohen, I. A. *J. Am. Chem. Soc.* **1976**, *98*, 6623–6628.
(2) (a) Schick, G. A.; Bocian, D. F. *J. Am. Chem. Soc.* **1980**, *102*, 7982–7984. (b) *Ibid.* **1983**, *105*, 1830–1838. (c) Schick, G. A.; Findsen, E. W.; Bocian, D. F. *Inorg. Chem.* **1982**, *21*, 2885–2887.
(3) (a) Kadish, K. M.; Cheng, J. S.; Cohen, I. A.; Summerville, D. A. *ACS Symp. Ser.* **1977**, *No. 38*, Chapter 5. (b) Kadish, K. M.; Bottomley, L. A.; Brace, J. G.; Winograd, N. J. *J. Am. Chem. Soc.* **1980**, *102*, 4341–4344. (c) Kadish, K. M.; Rhodes, R. K.; Bottomley, L. A.; Goff, H. M. *Inorg. Chem.* **1981**, *20*, 3195–3200.
(4) Bottomley, L. A.; Garrett, B. B. *Inorg. Chem.* **1982**, *21*, 1260.
(5) (a) English, D. R.; Hendrickson, D. N.; Suslick, K. S. *Inorg. Chem.* **1983**, *22*, 367–368. (b) Bocian, D. F.; Findsen, E. W.; Hofmann, J. A., Jr.; Schick, G. A.; English, D. R.; Hendrickson, D. N.; Suslick, K. S. *Inorg. Chem.* **1984**, *23*, 800–807. (c) English, D. R.; Hendrickson, D. N.; Suslick, K. S. *Inorg. Chem.* **1985**, *24*, 121–122.
(6) Tatsumi, K.; Hoffmann, R. J. *J. Am. Chem. Soc.* **1981**, *103*, 3328–3341.
(7) Ercolani, C.; Rossi, G.; Monacelli, F. *Inorg. Chim. Acta* **1980**, *44*, L215–L216.
(8) Ercolani, C.; Gardini, M.; Monacelli, F.; Pennesi, G.; Rossi, G. *Inorg. Chem.* **1983**, *22*, 2584–2589.
(9) Goedken, V. L.; Ercolani, C. *J. Chem. Soc., Chem. Commun.* **1984**, 378–379.

† Georgia Institute of Technology.
‡ Consiglio Nationale della Ricerche.

0020-1669/85/1324-3733$01.50/0

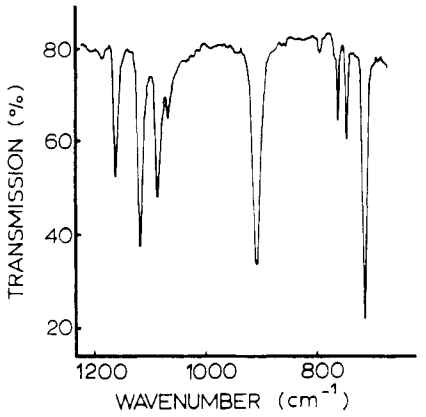

Figure 1. IR spectrum of $[(Pc)Fe]_2N$ over the spectral region 1200–600 cm^{-1}.

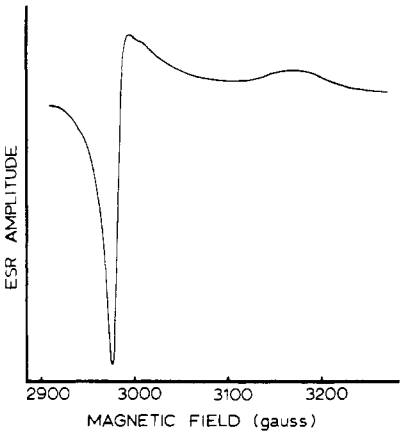

Figure 2. ESR spectrum of solid $[(Pc)Fe]_2N$ obtained at 77 K.

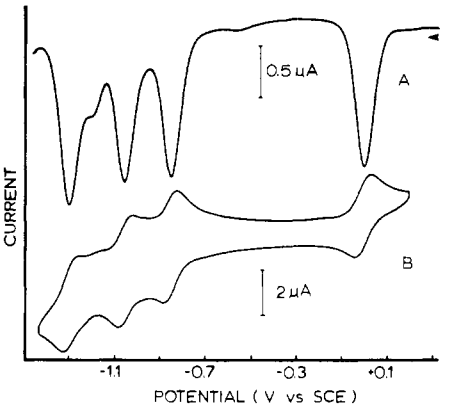

Figure 3. Voltammetric data obtained on a 0.269 mM solution of $[(Pc)Fe]_2N$ in pyridine. The upper trace (A) is a differential-pulse voltammogram taken at a potential sweep rate of 10 mV/s, a pulse amplitude of 25 mV, and a pulse frequency of 0.1 s. The lower trace (B) is a steady state cyclic voltammogram taken at a potential sweep rate of 200 mV/s.

cenium ion) were mixed together and this mixture was kept at constant stirring for 30 min. The reaction was heterogeneous with both the Pc reactant and product being insoluble. The reaction mixture was then filtered and the filter cake treated with a 10:1 acetonitrile/pyridine solution to dissolve the product as $([py)(Pc)Fe]_2N)PF_6$. The product was recovered by evaporation of the solvent; yield 50%.

Instrumentation. Voltammetric experiments were carried out with either an AMEL Model 472 multipolarograph or an IBM Instruments, Inc., Model EC225 polarographic system. A conventional three-electrode system was used with a Pt-button working electrode, a Pt-wire counter electrode, and a saturated calomel electrode (SCE) as reference. Aqueous contamination of electrochemical solutions from the reference electrode fill solution was minimized by isolating the reference electrode via a frit. Voltammograms were recorded on a Houston Omnigraphic 2000 X-Y recorded or on a Tektronix Model 564 storage oscilloscope. Scan rates ranged from 0.02 to 9.90 V/s for cyclic voltammetric experiments. Differential pulse voltammetric experiments were obtained with a potential scan rate of 10 mV/s. Pulse intervals varied between 0.1 and 0.5 s while pulse amplitudes varied between 5 and 100 mV.

All solutions were deoxygenated by passing a stream of solvent-saturated prepurified N_2 into the solution for at least 10 min prior to recording the voltammogram. To maintain an O_2-free environment, the solution was blanketed with N_2 during all experiments. All experiments were carried out at ambient temperature (23 ± 1 °C). All potentials reported herein were referenced to the SCE and were uncorrected for liquid-junction potentials. The uncertainty in each potential reported herein is ±10 mV. Spectral and spectroelectrochemical measurements were obtained with a Tracor Northern Optical multichannel analyzer system in the manner previously described.[10]

The supporting electrolyte, tetrabutylammonium perchlorate (TBAP) was obtained from the Eastman Chemical Co. Prior to use, TBAP was recrystallized in triplicate from absolute ethanol, dried in vacuo for 24 h at 100 °C, and stored in an evacuated desiccator. Pyridine was purchased from Mallinckrodt as reagent grade. This solvent was first treated with NaOH pellets, fractionally distilled from CaO under N_2, and then stored over 4A molecular sieves.

IR spectra of the complexes were measured in the region 4000–200 cm^{-1} with a Perkin-Elmer 621 spectrophotometer by suspending the samples as Nujol mulls between either NaI or NaCl plates.

Electron paramagnetic resonance spectra were recorded on a Varian E-12 spectrometer equipped with E-101 (for X-band spectra) microwave bridges. A Spectromagnetic Industries Model 5200 NMR Gaussmeter was used to measure the magnetic field.

Elemental analyses were performed by Atlantic Microlab, Inc., of Atlanta, GA.

Results and Discussion

A. Synthesis and Properties. The thermal decomposition of NaN_3 in the presence of either $[(Pc)Fe]_2O$ or (Pc)Fe in boiling α-chloronaphthalene yields $[(Pc)Fe]_2N$. The identification of the material as a μ-nitrido mixed-valence Fe^{III}–Fe^{IV} species rested on the following observations:[9] (1) The IR spectrum of the reaction product contained a new, very strong absorption at 915 cm^{-1} (Figure 1), which was assigned to the Fe–N–Fe antisymmetric stretching frequency. This is close to that observed in the $[(TPP)Fe]_2N$ complex[1] at 910 cm^{-1} (vs) and 885 cm^{-1} (m). (2) The X-ray powder pattern indicated that this species was isomorphous with $[(Pc)Fe]_2O$ (μ-oxo type II[8]) and also isomorphous with $[(Pc)Mn]_2O$ (obtained from the structurally characterized $[(py)(Pc)Mn]_2$ by heating the py adduct under vacuum).[8] (3) The ESR spectrum (Figure 2) obtained at 77 K on a solid sample of $[(Pc)Fe]_2N$ shows a typically axially symmetry spectrum ($g_\parallel$ = 2.03, $g_\perp$ = 2.13), consistent with a low-spin complex having an A_1 ground state. These parameters are similar to those observed for $[(TPP)Fe]_2N$[4] and appear to be indicative of extensive delocalization over the two iron centers. We are attempting a careful purification of the complex from the systematic presence of magnetic impurities, which lead to nonaccurate and nonreproducible values of the magnetic moment.

The complex is virtually insoluble in all noncoordinating solvents. Even in α-chloronaphthalene, only a faint blue color is observed. In the presence of nitrogenous bases such as pyridine, aliphatic amines, and diamines, the solubility is greatly enhanced, presumably because of some association of the amines with the vacant coordination sites.

The μ-nitrido dimer is also stable toward Fe–N–Fe bond dissociation and to redox reactions in the presence of amines. In this sense, it differs markedly from the corresponding μ-oxo dimer, which reverts to the $(Pc)Fe^{II}(amine)_2$ when amines are added to the solutions. Long-term standing of these solutions in the presence of dioxygen leads to a small amount of oxidation to the cationic species $([(Pc)Fe]_2N)^+$ as shown from the changes in the visible spectrum. The same cationic species can be obtained electrochemically or chemically by oxidation with the ferrocenium cation. The increase of charge on the dimeric species has two immediate effects: (1) it increases the affinity for axial ligands that are now associated with the complex when isolated, and (2) the formation

(10) Bottomley, L. A.; Deakin, M. R.; Gorce, J.-N. *Inorg. Chem.* **1984**, *23*, 3563–3571.

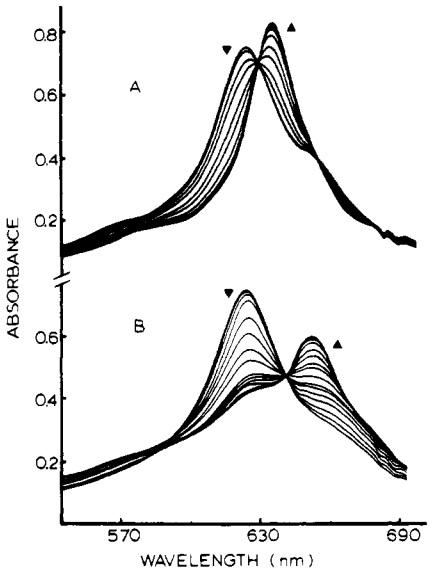

Figure 4. Visible spectra obtained during the electrolysis of a 0.937 mM solution of $[(Pc)Fe]_2N$ in pyridine at the OTTLE. Part A depicts the spectra obtained when the applied potential was stepped from −0.20 to +0.30 V, generating the dimeric cation. Part B depicts the spectra obtained after the applied potential was stepped from −0.20 to −0.93 V, generating the dimeric anion.

of the salt greatly increases the solubility of the complex.

B. Electrochemistry of $[(Pc)Fe]_2N$. Electrooxidation of $[(Pc)Fe]_2N$. Figure 3 depicts typical voltammograms obtained for $[(Pc)Fe]_2N$ dissolved in pyridine that was 0.1 M in TBAP. Sweeping the potential positive of E_{oc} (−0.50 V) located only one electrooxidative process within the accessible solvent potential range. Both variable potential sweep cyclic voltammetry and variable pulse amplitude differential pulse voltammetry were employed to evaluate the electrochemical mechanism of the oxidation processes. Analysis of the cyclic voltammetric data for the first oxidation produced the following trends: (a) $E_{1/2}$ (at 0.00 V) and $E_{p,a/2}$ (at −0.03 V) remained constant regardless of potential sweep rate; (b) $i_{p,c}/V^{1/2}$ was independent of sweep rate; (c) the current ratio $i_{p,a}/i_{p,c}$ was unity and independent of the potential sweep rate; (d) the potential separation between the anodic and cathodic peaks was measured as 63 ± 1 mV at a potential sweep rate of 20 mV/s and increased with increasing sweep rate; (e) the anodic peak shape ($E_{p,a} - E_{p,a/2}$) was 32 ± 3 mV at all sweep rates.

Analysis of the differential pulse data produced the following trends: (a) $E_{1/2}$ values were identical with those obtained in the cyclic voltammetric experiments and were independent of the pulse amplitude; (b) $W_{1/2}$ values decreased with decreasing pulse amplitude to a value of 95 mV at a pulse amplitude of 10 mV (c) $i_{p(+)}/i_{p(-)}$ were unity over the entire range of pulse amplitudes employed; (d) $E_{p(+)} - E_{p(-)}$ values were consistently 2 mV less than the pulse amplitude setting. Taken collectively, the voltammetric results indicated that the first oxidation involved the reversible abstraction of one electron per dimer. Spectroelectrochemical and coulometric experiments were carried out to confirm this assignment.

A 0.937 mM solution of $[(Pc)Fe]_2N$ in 0.1 M TBAP/pyridine gave a spectrum characteristic of the nitrido-bridged iron phthalocyanine dimer with a strong absorption band at 626 nm (ϵ 5.25 × 10^4) and two shoulders at 573 (ϵ 1.25 × 10^4) and 658 nm (ϵ 1.82 × 10^4). A potentiometric chronoabsorptometric experiment carried out at an applied potential of +0.300 V resulted in the spectral changes depicted in Figure 4A. A final spectrum of the product was obtained within 40 s. It was characterized by an absorption band at 637 nm and two shoulder bands at 578 and 677 nm. The spectral interconversion produced well-defined isosbestic points at 502, 631, 658, and 677 nm. Reversal of the applied potential to −0.200 V completely regenerated the starting material. Isosbestic points were observed at the same wavelengths corresponding to those observed during the oxidative step.

On a fresh solution of $[(Pc)Fe]_2N$, a multiple potential step chronoabsorptometric experiment was performed. The spectral changes observed were identical with those depicted in Figure 4. Nernst plots were constructed from the absorbance changes measured at 626 and 637 nm. The linear traces obtained indicated the chemically reversible passage of one electron per dimer at a formal potential of 0.00 V.

Electroreduction of $[(Pc)Fe]_2N$. Sweeping the electrode potential negative of E_{oc} located three electron-transfer processes within the accessible range of the solvent. Analysis of the results from variable potential sweep rate cyclic voltammetric and variable pulse amplitude differential pulse voltammetric experiments (in the manner detailed above for the oxidation process) for the first reduction process indicated that the dimer is reversibly reduced at $E_{1/2}$ = −0.83 V. The second and third electroreduction processes, occurring at −1.02 and −1.29 V, respectively, were reversible at moderate to fast potential sweep rates. At slow potential sweep rates, two additional processes were observed at $E_{p,a}$ values of −0.93 and −1.15 V, respectively at a sweep rate of 100 mV/s. This finding indicated that the dimer dianion and trianion underwent chemical reactions following the charge-transfer step.

To assess the temporal stability of the reduced forms of the dimer a 0.937 mM solution of $[(Pc)Fe]_2N$ in pyridine was placed in an OTTLE. A potentiostatic chronoabsorptometric experiment carried out at an applied potential of −0.93 V resulted in the spectral changes depicted in Figure 4B. A final spectrum of the product was obtained with 40 s. It was characterized by an absorption band at 655 nm and two shoulder bands at 590 and 627 nm. The spectral interconversion produced a well-defined isosbestic point at 640 nm. This species was stable under an applied potential for at least 2 h. Reversal of the applied potential to −0.65 V completely regenerated the starting material. A controlled-potential electrolysis experiment carried out at −0.93 V indicated the passage of 1.00 ± 0.05 electron per dimer.

When the potential of the Pt-minigrid electrode was stepped from −0.93 to −1.16 V, a rapid spectral change occurred within 30 s. New bands grew at 516 and 594 nm, and the intense absorption at 655 nm underwent a slight wavelength shift to 658 nm. Over the next 3 min the 516-nm band grew to an absorbance twice that of the original band at 655 nm, the band at 594 nm shifted to 598 nm, and the 658-nm band decreased in absorbance and shifted to 663 nm. The transition did not occur with isosbestic points. The latter spectrum is identical with that of the monomeric anion $[(Pc)Fe]^-$. Attempts to regenerate the spectrum of the starting material were futile. Stepping the electrode potential back to −0.40 V produced the characteristic spectrum of the monomer, (Pc)Fe. A controlled-potential electrolysis experiment carried out at −1.16 V indicated passage of 4.9 ± 0.2 electrons per dimer.

Electrode Reactions of $[(TPP)Fe]_2N$. To permit comparison of the electrode mechanisms between the two known μ-nitrido iron dimers, the electrochemistry of $[(TPP)Fe]_2N$ was investigated under the same conditions as employed for $[(Pc)Fe]_2N$. Kadish and co-workers[3] have previously characterized the voltammetry of this compound in CH_2Cl_2. Their electrochemical measurements have demonstrated that up to four electrons may be extracted from, or one electron added to the molecule without destruction of the dimeric structure. They suggesed that a similar electron-transfer pathway existed in benzonitrile. Potentials were given for the first oxidation and first reduction of $[(TPP)Fe]_2N$ in pyridine, but no other data was provided.

Sweeping the potential of E_{oc} (−0.46 V) located only one electrooxidation ($E_{1/2}$ = 0.26 V) whereas sweeping negatively from E_{oc} located up to five processes within the accessible solvent potential range, the number observed depending upon the switching potential. Figure 5 depicts several cyclic voltammograms obtained on a solution of $[(TPP)Fe]_2N$ with the potential sweep originating at 0.5 V. Scans A and B in this figure show that the transition from dimer cation to dimer anion occurred in two steps without dimeric decomposition. It is only after the second reduction of the dimer that the cyclic voltammogram indicated the presence of monomeric material at the electrode. In scans C–E, the two

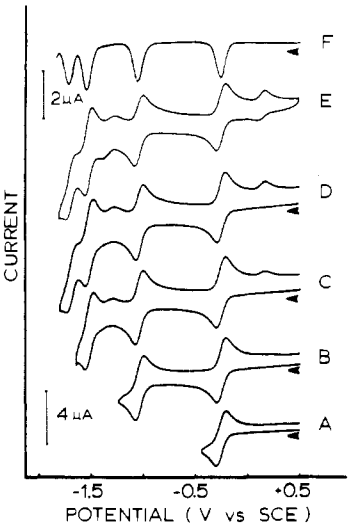

Figure 5. Cyclic voltammograms obtained on a 0.25 mM solution of $[(TPP)Fe]_2N$ dissolved in pyridine at a potential sweep rate of 200 mV/s and at the following switching potentials: (A) −0.47 V; (B) −1.28 V; (C) −1.62 V; (D) −1.77 V; (E) −1.77 V. Traces A–D were first-scan cyclic voltammograms whereas trace E is a steady-state cyclic voltammogram. Trace F is a differential-pulsed voltammogram obtained under the experimental conditions listed in the caption for Figure 3.

Table I. Midpoint Potentials (V) for the μ-Nitrido Dimers of Phthalocyanine and Tetraphenylporphyrin in Pyridine

redox reacn[a]	$[(Pc)Fe]_2N$	$[(TPP)Fe]_2N$
+1/0	0.00	−0.25
0/−1	−0.83	−1.04
−1/−2	−1.02	−1.52
−2/−3	−1.29	−1.69

[a] Denotes charge on the dimer for the electrode reactant and electrode product.

new anodic processes at $E_{p,a} = -1.26$ and 0.17 V are voltammetric fingerprints of monomeric (TPP)Fe. The observed currents were found to be inversely proportional to the potential sweep rate. Analysis of the variable sweep rate cyclic voltammetric data and the variable pulse amplitude differential pulse data indicated Nernstian behavior for the first-oxidation and first-reduction processes ($E_{1/2} = -0.25$ and −1.04 V, respectively). The second and third electroreductions ($E_{1/2} = -1.52$ and −1.69 V) were coupled to chemical reactions after the charge-transfer step. Table I lists the midpoint potentials observed for both $[(TPP)Fe]_2N$ and $[(Pc)Fe]_2N$ in pyridine.

To ascertain the temporal stability of the electrode products, potentiostatic chronoabsorptometric experiments were performed in the same manner as described above for $[(Pc)Fe]_2N$ with comparable results. Potentiostating the OTTLE at 0.00 V produced a smooth spectral transition from $[(TPP)Fe]_2N$ to $([(TPP)Fe]_2N)^+$. Similarly, potentiostating the OTTLE at −1.30 V generated the spectrum of $([(TPP)Fe]_2N)^-$. Both products were stable for hours under the applied potential. Their pertinent spectral features are listed in Table II. Potentiostating the OTTLE negative of the second reduction ($E_{appl} < -1.52$ V) generated spectra[11] characteristic of $[(TPP)Fe(py)_x]^-$. A controlled-potential electrolysis at −1.65 V required the passage of 5 equiv of charge/dimer.

Electron-Transfer Pathways. On the basis of the electrochemical results presented, the electron-transfer reactions of $[(Pc)Fe]_2N$ and $[(TPP)Fe]_2N$ can be accounted for by Schemes I and III, respectively. The midpoint potentials for each electron-transfer reaction are given above the reaction and the superscripted Roman numerals denote the formal valences assigned to each of the Fe atoms. The electron-transfer reactions of monomeric (Pc)Fe and (TPP)Fe have been accounted for by previous investigators.[13,14] Their pathways are listed below as Schemes II and IV for ready comparison. For clarity, axially coordinated solvent molecules have been omitted. For comparison, the redox potentials measured for both μ-nitrido dimers are listed in Table I.

Table II. Visible Spectral Data for the μ-Nitrido Dimers of Phthalocyanine and Tetraphenylporphyrin in Pyridine

dimer	charge[a]	wavelength,[b] nm (ε × 10⁴)		
Pc	+1	574 s (1.18)	634 (5.76)	648 s (3.00)
	0	537 s (1.24)	626 (5.25)	658 s (1.82)
	−1	594 s (1.77)	627 s (2.98)	655 (4.26)
TPP	+1	415 (19.2)	541 (1.40)	578 (1.00)
				624 s (0.70)
	0	387 s (9.60)	408 (20.4)	532 (1.30)
				617 s (0.40)
	−1	404 (31.6)	522 (1.30)	553 (1.00)
				613 (0.50)

[a] Solution was 0.2 M in the supporting electrolyte TBAP. [b] s denotes wavelength of a shoulder.

Scheme I. Electrode Mechanism for $[(Pc)Fe]_2N$

$$([(Pc)Fe^{IV,IV}]_2N)^+ + e^- \xrightleftharpoons{0.00\ V} [(Pc)Fe^{III\,1/2,III\,1/2}]_2N$$

$$[(Pc)Fe^{III\,1/2,III\,1/2}]_2N + e^- \xrightleftharpoons{-0.83\ V} ([(Pc)Fe^{III,III}]_2N)^-$$

$$([(Pc)Fe^{III,III}]_2N)^- + e^- \xrightleftharpoons{-1.02\ V} ([(Pc)Fe^{II\,1/2,II\,1/2}]_2N)^{2-}$$

$$([(Pc)Fe^{II\,1/2,II\,1/2}]_2N)^{2-} + e^- \xrightleftharpoons{-1.29\ V} ([(Pc)Fe^{II,II}]_2N)^{3-}$$

at slow potential sweep rates or long times the pathway for dimer decomposition was potential dependent:

at $-1.02 \geq E \geq -1.21$ V

$$([(Pc)Fe^{II\,1/2,II\,1/2}]_2N)^{2+} + 3e^- \rightarrow 2[(Pc)Fe^{I}]^- + NH_x^{x-3}$$

at $-1.21 \geq E \geq -1.29$ V

$$([(Pc)Fe^{II\,1/2,II\,1/2}]_2N)^{2-} + 5e^- \rightarrow 2[(Pc)Fe^{I}]^{2-} + NH_x^{x-3}$$

at $E < -1.29$ V

$$([(Pc)Fe^{II,II}]_2N)^{3-} + 4e^- \rightarrow 2[(Pc)Fe^{I}]^{2-} + NH_x^{x-3}$$

Scheme II. Electrode Mechanism for (Pc)Fe

$$(Pc)Fe^{II} + e^- \xrightleftharpoons{-0.96\ V} [(Pc)Fe^{I}]^-$$

$$[(Pc)Fe^{I}]^- + e^- \xrightleftharpoons{-1.21V} [(Pc)Fe^{I}]^{2-}$$

Scheme III. Electrode Mechanism for $[(TPP)Fe]_2N$

$$([(TPP)Fe^{IV,IV}]_2N)^+ + e^- \xrightleftharpoons{-0.25\ V} [(TPP)Fe^{III\,1/2,III\,1/2}]_2N$$

$$[(TPP)Fe^{III\,1/2,III\,1/2}]_2N + e^- \xrightleftharpoons{-1.04\ V} ([(TPP)Fe^{III,III}]_2N)^-$$

$$([(TPP)Fe^{III,III}]_2N)^- + e^- \xrightleftharpoons{-1.52V} ([(TPP)Fe^{II\,1/2,II\,1/2}]_2N)^{2-}$$

$$([(TPP)Fe^{II\,1/2,II\,1/2}]_2N)^{2-} + e^- \xrightleftharpoons{-1.69\ V} ([(TPP)Fe^{II,II}]_2N)^{3-}$$

at slow potential sweep rates or long times the pathway for dimer decomposition was potential dependent:

at $-1.52 \geq E \geq -1.69$ V

$$([(TPP)Fe^{II\,1/2,II\,1/2}]_2N)^{2-} + 3e^- \rightarrow 2[(TPP)Fe^{I}]^- + NH_x^{x-3}$$

at $E < -1.69$ V

$$([(TPP)Fe^{II,II}]_2N)^{3-} + 4e^- \rightarrow 2[(TPP)Fe^{I}]^{2-} + NH_x^{x-3}$$

(11) Clack, D. W.; Yandle, J. R. *Inorg. Chem.* **1972**, *8*, 1738–1742.
(12) Reed, C. A. *Adv. Chem. Ser.* **1982**, *No. 201*, Chapter 15.
(13) Lever, A. B. P.; Licoccia, S.; Magnell, K.; Minor, P. C.; Ramaswamy, B. S. *Adv. Chem. Ser.* **1982**, *No. 201*, Chapter 11 and references therein.
(14) Bottomley, L. A.; Kadish, K. M. *Inorg. Chem.* **1981**, *20*, 1348–1357.

Scheme IV. Electrode Mechanism for (TPP)Fe

$$[(TPP)Fe^{III}]^+ + e^- \overset{+0.18\ V}{\rightleftharpoons} (TPP)Fe^{II}$$

$$(TPP)Fe^{II} + e^- \overset{-1.32\ V}{\rightleftharpoons} [(TPP)Fe^{I}]^-$$

$$[(TPP)Fe^{I}]^- + e^- \overset{-1.70\ V}{\rightleftharpoons} [(TPP)Fe^{I}]^{2-}$$

$[(TPP)Fe]_2N$ has previously been given the unusual assignment of $III^1/_2$ based upon the results from Mössbauer,[1,5] ESCA,[3b] and EPR[4] experiments. As $[(Pc)Fe]_2N$ yields comparable EPR[9] and electrochemical activity, the formal valences of the Fe atoms are similarly assigned. The oxidation of the two μ-nitrido dimers yields diamagnetic complexes with two equivalent Fe(IV) centers. This assignment has been clearly established by Mössbauer and NMR experiments.[3c,5c,9]

For all four electron transfers, the reduction of the phthalocyanine complex occurs at more positive potentials as compared to the reduction of the TPP complex. This is in accord with expectations; the more basic the macrocycle, the more negative the reduction potential. For both dimers, only the first reduction process is free from the complicating effects of dimer decomposition. We have assigned these electroreductions as metal-centered electron-transfer reactions in accordance with the MO diagram put forth for these complexes.[6] The HOMO in these dimers is an A_1 orbital comprised of the in-phase and out-of-phase combinations of the N 2s and Fe d_{z^2} atomic orbitals. The LUMO is an e_1 orbital derived from the N 2p and Fe d_{xz} and d_{yz} atomic orbitals. The first electroreduction pairs the electron residing in the A_1 orbital, producing two Fe(III) centers. The expected change in the electronic spectrum for a metal-centered reduction is a red shifting in the Soret and visible bands with an increase in the intensity of the Soret band. This is indeed observed.

Subsequent reductions populate the antibonding e_1 orbital and destabilize the dimeric linkage. We have assigned the dianion for both dimers as an $Fe^{II\,1/2}$–N–$Fe^{II\,1/2}$ species. This assignment assumes that the extent of electron delocalization present in the neutral complex does not significantly differ from that present in the dianion. The ultimate reduction products (the monomers) are designated in accordance with the findings of Reed[12] for the porphyrin complex and of Lever[13] for the phthalocyanine complex.

For both μ-nitrido complexes, decomposition of the dimeric structure frees an N^{3-} species. This species is probably hydrolyzed by adventitious water present in the supporting electrolyte to form NH_3 or NH_2^-. Experiments are presently under way to determine the fate of the bridging moiety after multielectron transfer.

Acknowledgment. L.A.B. acknowledges the Istituto di Teoria e Struttura Elettronica, CNR, Area della Ricerca di Roma (Montelibretti), and V.L.G. acknowledges the Chemistry Department of the University of Rome for visiting professorships and kind hospitality. We thank Paul Wojciechowski for his assistance in obtaining the EPR data and Professor Craig Hill for helpful discussions.

Registry No. $[(Pc)Fe]_2N$, 98395-07-4; (Pc)Fe, 132-16-1; $([(py)(Pc)Fe]_2N)PF_6$, 98395-09-6; $[(TPP)Fe]_2N$, 59114-43-1; $[(Pc)Fe]_2N^+$, 98395-10-9; $[(Pc)Fe]_2N^-$, 98395-11-0; $[(Pc)Fe]_2N^{2-}$, 98395-12-1; $[(Pc)Fe]_2N^{3-}$, 98395-13-2; $[(TPP)Fe]_2N^+$, 78591-88-5; $[(TPP)Fe]_2N^-$, 98395-14-3; $[(TPP)Fe]_2N^{2-}$, 98395-15-4; $[(TPP)Fe]_2N^{3-}$, 98395-16-5; NaN_3, 26628-22-8.

Contribution from the Departments of Chemistry, Massachusetts Institute of Technology, Cambridge, Massachusetts 02139, and Columbia University, New York, New York 10027

Copper(II) Tropocoronands: Synthesis, Structure, and Properties of Mononuclear Complexes

WILLIAM M. DAVIS,† ARIE ZASK,‡ KOJI NAKANISHI,‡ and STEPHEN J. LIPPARD*†

Received February 27, 1985

The synthesis of four mononuclear copper(II) tropocoronands, [Cu(TC-*n*,*n*′)] (*n*,*n*′ = 3,3; 4,4; 4,5; 5,5), is described. Tropocoronands are a new class of metal-complexing macrocycles derived from two aminotropone imine moieties connected by two polymethylene linker chains of lengths *n* and *n*′. The complexes [Cu(TC-3,3)], [Cu(TC-4,4)], and [Cu(TC-5,5)] have been structurally characterized by X-ray crystallography. The geometry at the copper center smoothly distorts from planar (tetrahedral twist angle $\theta = 0°$) toward tetrahedral (twist angles $\theta = 36.6$ and 61.3°, respectively) along this series. Molecular mechanics calculations reveal the tetrahedral twist to result from relief of unfavorable steric interactions within the polymethylene linker chains as *n* increases. The smooth variation in θ with *n* for copper(II) tropocoronands contrasts with previous results for the corresponding nickel(II) complexes where the transition was discontinuous owing to an additional electronic barrier to the conversion from planar, $S = 0$, to tetrahedral, $S = 1$, stereochemistry. No such change in spin state can occur for copper(II). The variation in electronic structures of all four copper(II) tropocoronand complexes in solution is manifest by striking, if predictable, changes in electron spin resonance spectral parameters and optical spectroscopic (d–d) absorption bands. The solid-state magnetic susceptibilities of the four [Cu(TC *n*,*n*′)] complexes, measured by SQUID susceptometry down to 5–10 K, are reported. [Cu(TC-3,3)], $CuC_{20}H_{22}N_4$, crystallizes in the monoclinic system, space group $P2_1/n$, $a = 9.933$ (1) Å, $b = 5.798$ (1) Å, $c = 14.520$ (2) Å, $\beta = 91.82$ (1)°, and $Z = 2$; [Cu(TC-4,4)], $CuC_{22}H_{26}N_4$, crystallizes in the monoclinic system, space group $P2_1/c$, $a = 11.178$ (2) Å, $b = 8.636$ (1) Å, $c = 20.188$ (8) Å, $\beta = 90.39$ (2)°, and $Z = 4$; [Cu(TC-5,5)], $CuC_{24}H_{30}N_4$, crystallizes in the hexagonal system, space group $P6_522$, $a = b = 11.044$ (2) Å, $c = 30.390$ (3) Å, and $Z = 6$.

Introduction

Recently we have been exploring the coordination chemistry of the tropocoronands H_2(TC-*n*,*n*′), a new class of ligands derived from aminotropone imines.[1,2] In the case of [Ni(TC-*n*,*n*′)] complexes, increasing the numbers of methylene groups (*n*,*n*′) in the two linker chains resulted in distortion of the stereochemistry at the metal center from planar, twist angle $\theta = 0°$, toward tetrahedral, $\theta = 90°$. For Ni(II) the planar-to-tetrahedral transition is accompanied by a change in electronic spin state from $S = 0$ to $S = 1$. As a consequence, the distortion of the nickel(II) tropocoronands from planar to tetrahedral is discontinuous, with the changeover occurring between [Ni(TC-4,5)] ($S = 0$, θ =

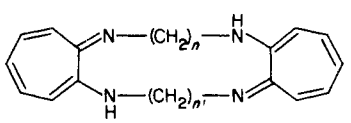

H_2(TC-*n*,*n*′)
n,*n*′ = 3,3; 4,4; 4,5; 5,5; 6,6

† Massachusetts Institute of Technology.
‡ Columbia University.

(1) (a) Imajo, S.; Nakanishi, K.; Roberts, M.; Lippard, S. J.; Nozoe, T. *J. Am. Chem. Soc.* **1983**, *105*, 2071. (b) Zask, A.; Gonnella, N.; Nakanishi, K.; Turner, C. J.; Imajo, S.; Nozoe, T., to be submitted for publication.
(2) Davis, W. M.; Roberts, M. M.; Zask, A.; Nakanishi, K.; Nozoe, T.; Lippard, S. J. *J. Am. Chem. Soc.* **1985**, *107*, 3864.

0020-1669/85/1324-3737$01.50/0